Int. J. Dev. Biol. 42: 79-85(1998)

Morphological evidence for a morphogenetic field in gastropod mollusc eggs

SHEENA E.B. TYLER, RONALD D. BUTLER and SUSAN J. KIMBER*

School of Biological Sciences, University of Manchester, Manchester, United Kingdom

ABSTRACT Eggs of the marine gastropod *Crepidula fornicata* examined by confocal imaging of FITC-lectin binding to the surface, and cryoscopic-SEM both reveal a surface architecture of linear structures organized around the animal-vegetal axis, which is spatially related to the anterior-posterior (a-p) axis of the subsequent embryo. A series of structures is also orientated with reference to specific micromere quartets formed during spiral cleavage. Thus, the surface architecture may provide a visible marker for a morphogenetic field which generates the a-p axis and organizes the cleavage pattern. Moreover, this architecture is co-extensive with that found on the vegetal, polar lobe-bearing region of eggs, as described by others, and which varies between gastropod taxa with varied types of body form. Confocal imaging reveals a distinct localization of F-actin to the architecture of the lobe region. However, the integrity of this F-actin is not responsible for the maintenance of the surface architecture. The significance of these findings to our understanding of the generation of diversity within the Gastropoda and general ontogenic mechanisms is discussed.

KEY WORDS: *mollusc egg, morphogenetic field, polarity, polar lobe*

Introduction

In molluscs, generation of the three body axes is reflected in the cleavage pattern. Thus, successive cleavage quartets are organized around the animal-vegetal axis, which is spatially-related to the anterior-posterior (a-p) or primary axis of the embryo: the animal pole corresponds with the cephalic or anterior pole, and the vegetal pole corresponds with the caudal or posterior pole (Van den Biggelaar and Guerrrier, 1983). In eggs with polar lobe formation, the dorso-ventral, or second axis, is generated by specification of the D cell as the dorsal quadrant. This specification results from inheritance of materials at the vegetal pole of the egg transferred via the polar lobe (reviewed by Verdonk and Cather, 1983). Subsequent to the development of the dorso-ventral axis, the asymmetrical structure, or tertiary axis of the gastropod body form results from a ventral flexion (correlating with shell field evagination), and a posterior torsion (Raven, 1966). An initial asymmetry is suggested by a right or left displacement of the shell field (shell gland), or even earlier, when the 5c cell from the fifth micromere quartet is displaced dorsally, and the 5d cell medioventrally.

There is evidence from a number of developmental systems that the plasma membrane and cortex of the cells are involved in axis establishment (Nuccitelli, 1988). If this is so, it should be possible to detect cell surface asymmetries associated with these axes of polarity (Nuccitelli, 1984). This is indeed evident in mollusc eggs, which show an animal-vegetal polarity in the distribution of various components, including the architecture of the cell surface, the distribution of inner membrane particles in the plasma membrane, membrane fluidity characteristics, and plasma membrane ionic conductance properties (reviewed in Dohmen, 1992). A clear demonstration of the regional differentiation at the vegetal pole is provided by the striking differences revealed by scanning electron microscopy (SEM) in surface architecture between the vegetal pole area and the rest of the egg surface in certain polar lobe-forming gastropod eggs such as those of *Buccinum, Crepidula* and *Nucella* (Dohmen and van der Mey, 1977). The vegetal pole is characterized by ridges of microvilli. The ridges are arranged in a species-specific pattern. The vegetal surface architecture in *Crepidula* was also revealed with FITC-conjugated Conconavalin A lectin (Dohmen, 1992). Dohmen suggested that the ridges provide an increased surface area accommodating more lectin-binding receptors, enabling the ridges to be clearly delineated.

Abbreviations used in this paper: EGTA, ethylene glycol-bis [B-aminoethylether] N,N,N',N'-tetraacetic acid; GSL-1, *Griffonia (Bandeirea) simplicifolia* lectin-1; LT-SEM, low temperature SEM; PIPES, piperazine-N,N'-bis [2-ethanesulphonic acid]; AB-FSW, sodium azide and bovine serum albumen in filtered seawater; vm, vitelline membrane.

***Address for reprints:** School of Biological Sciences, Stopford Building, University of Manchester, Oxford Road, Manchester, M13 9PT, UK. FAX: 0161-275-3915. e-mail: Sue.Kimber@man.ac.uk

0214-6282/98/$10.00

Printed in Spain

This paper further investigates the potential developmental significance of this surface architecture. Firstly, this has involved novel methods to reveal more information on the nature of surface detail, and secondly, its extent over the egg. In the SEM study undertaken by Dohmen and van der Mey (1977), eggs were prepared by the critical-point drying method. Fixation in osmium tetroxide and dehydration may lead not only to dehydration shrinkage but other deleterious effects. These may impair, distort or even obliterate significant egg surface features. Such preparation stages were obviated in this study by employing low temperature SEM (LT-SEM). In addition, FITC-lectin labeled eggs were examined by confocal imaging microscopy. Thirdly, FITC-lectins also have been utilized to determine tempero-spatial attributes of the surface architecture. Fourthly, a cause-effect relationship between the surface architecture and the underlying cytoskeleton was investigated: particularly how does the distribution of F-actin, essential for lobe formation in *Nassarius* (Speksnijder *et al.*, 1991), relate to that of the surface architecture? This was examined using FITC-conjugated phalloidin and cytochalasin D for respectively the detection and disruption of F-actin.

Results

FITC-GSL-1 staining resulted in a superficially uniform fluorescence over the surface of uncleaved eggs, 2-cell, 4-cell, 8-cell, 12-cell, 16-cell, 24-cell, and 40+ cell stages, except for the texture of a distinct architecture which was reflected in the pattern of fluorescence. This surface architecture consisted of series of parallel lines or ridges, with some bifurcations and mergings, and was prominent on the animal surface and the polar lobe. It persisted on at least some cells until gastrulation (ie. blastopore formation) and to subsequent post-gastrulation stages (in preparation). It is uncertain as to whether the GSL-1 binds the plasma membrane, the overlying vitelline membrane (vm), or an extracellular matrix between the two. However, the pattern of the vm very closely resembles that of the surface, because the former is so closely applied to the latter (Dohmen and Van der Mey, 1977). Therefore the lectin binding serves as a marker of the surface architecture pattern irrespective of its specific morphological site of binding. It is also thus very likely that the surface architecture pattern resides on the surface, not just on the overlying vitelline membrane.

Animal region surface architecture

At the 4-cell stage, the first to be examined in detail, a characteristic series of fluorescent lines was apparent on the animal region of each cell. This pattern continued to be seen at least to the 12-cell and 16-cell stages. Using confocal imaging, the pattern of surface architecture depicted by GSL-1 staining was most clearly observed at the 16-cell stage (Fig. 1A and B). Because the pattern is similar for each quadrant, it will only be described for one of them (the upper right quadrant annotated in Fig. 1B), with the distribution of lines on each of the cells in this quadrant being considered in turn.

On the $1q^1$ cell, near the lateral boundary between the adjacent $1q^1$ cells, the lines moved radially outwards from the animal pole (Fig. 1B, short arrows). Lines located in the central region of $1q^1$ curved away from the animal pole (Fig. 1B, long arrows). In the distal circumferential region near the cell boundary between $1q^1$ and $1q^2$, lines ran parallel to that boundary.

Lines on the $1q^2$ cell were continuous with both those on $1q^1$ and those on the $1q^1$ and 2q cells in the dextral neighboring quadrant. On $1q^2$, these lines ran in parallel, and continued radially outwards from the animal pole.

On the 2q cell, lines formed a parallel series tangential to the animal pole, and continued on to lateral neighboring cells. In addition, a series of concentric lines was evident, arranged around a centre of radius (open arrows on Fig. 1B).

Parallel lines continuous with those on 2q and $1q^2$ passed radially away from the animal pole over Q, curving dextrally as they did so (curved arrow on Fig. 1B), and forming a centre of radius (open arrow on Fig. 1B) on Q. More distally on Q, lines spanned the circumference, generally tangential to the animal pole.

The 16-cell stage observed with LT-SEM (Fig. 2A and 2B) displayed a surface architecture consisting of ridged structures, branching over the surface of the micromeres and macromeres and organized into orientated linear arrays. This pattern can be

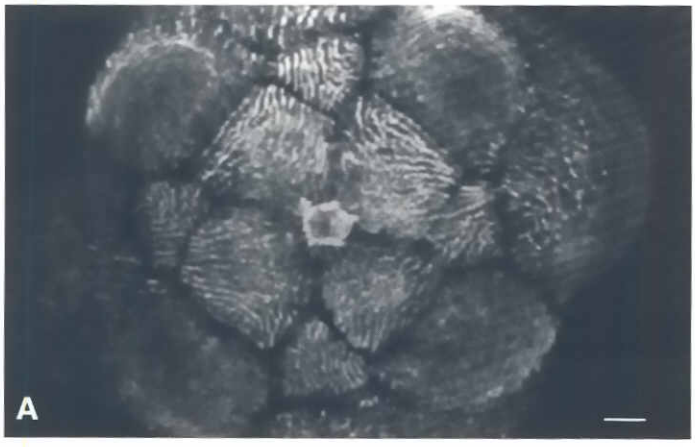

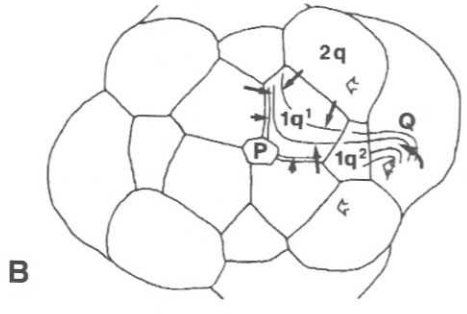

B

Fig. 1. (A) Live 16-cell stage embryo stained with FITC-GSL-1. *Confocal image of animal region showing surface architecture pattern. Bar, 20 μm.* **(B)** *Diagram of Figure 1A, denoting detail of upper right quadrant. Micromere cells: $1q^1$ and $1q^2$, daughter cells of 1st quartet; 2q, 2nd quartet. Q, macromere quartet. Open arrows indicate position of centres of radius. Relationship of surface architecture lines to animal-vegetal axis passing through polar body (P): some lines originate from pole (short arrow); other lines pass away from pole (long arrow). Lines passing on to Q cell curve dextrally (curved arrow).*

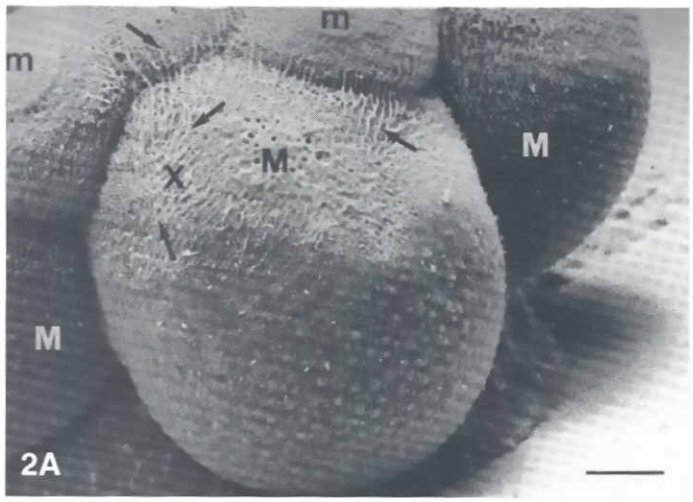

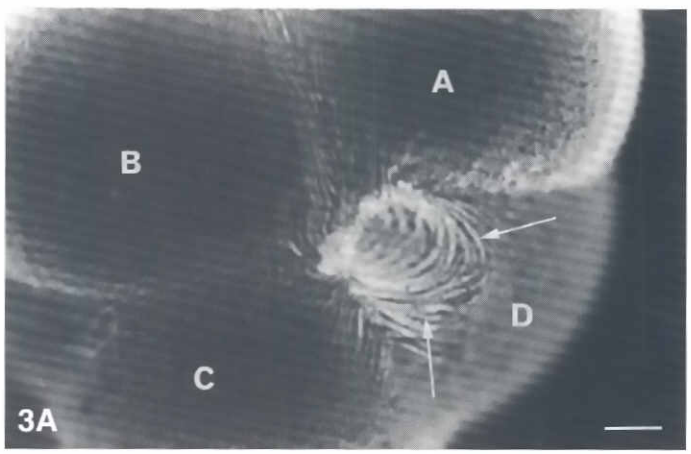

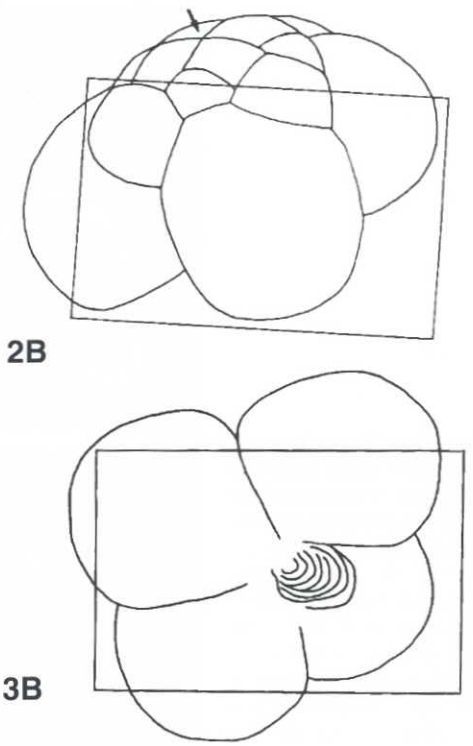

Fig. 2. (A) Low temperature SEM image of 16-cell stage embryo: *note surface architecture (arrowed) overlying micromeres (m) and macromeres (M). Lines on region X correlate with those on Q cell of Figures 1A and 1B. Bar, 25 μm.* **(B)** *Diagram showing side view of embryo at 16-cell stage. Boxed area denotes field of view shown in Fig. 2A. Arrow indicates location of animal pole.*

Fig. 3. (A) Live 4-cell stage embryo stained with FITC-GSL-1. *Confocal image of vegetal surface architecture (arrowed) on polar lobe. Letters denote A, B, C and D cells. Bar, 15 μm.* **(B)** *Diagram of ventral surface at 4-cell stage, with slight oblique tilt. Boxed area denotes field of view shown in Fig. 3A.*

correlated with the surface patterning seen with fluorescent lectins (Fig. 1A and B). Thus, the lines on region X of Figure 2A correlate specifically with the dextral curving series of lines on the Q cell of Figure 1B (Fig. 1B, curved arrow).

Comparison of LT-SEM images of *Crepidula* with published SEM observations from conventional critical-point dried eggs shows that both techniques reveal similar structures. These structures include the characteristic vegetal surface architecture on eggs of *Crepidula* (Dohmen and van der Mey, 1977). However, there are additional features uniquely attributable to the LT-SEM method, including surface architecture overlying the animal region which is of similar topography to the pattern seen using FITC-lectins. The LT-SEM study therefore confirms that the lectin-binding patterns are not merely a biochemical phenomenon expressed on a relatively structureless surface. Conventional SEM studies (Craig and Morrill, 1986) showed the presence of surface folds surrounding the micromeres of *Ilyanassa* eggs at the 8-cell stage, and it was suggested that these folds were indicative of ongoing cytokinesis. The published illustrations show a faint surface architecture of ridges swirling over the macromeres, reminiscent of that seen in *Crepidula* (Fig. 2A). The processing of eggs for conventional SEM may thus impair much of the animal region surface architectural detail. Further studies are needed to compare the animal region surface architecture of *Crepidula* and/or *Ilyanassa* eggs observed by critical-point drying and LT-SEM.

Vegetal surface architecture

The architecture overlying the micromeres is co-extensive with that found on the vegetal surface (Fig. 3A and B) similar to observations by Dohmen (1992) using fluorescent lectins without confocal imaging, and persists at least until gastrulation, when cells undergo ingression away from the surface (Fig. 4A). Gastrulating embryos incubated simultaneously with FITC-GSL-1 and cytochalasin D (Fig. 4B-D) showed a fluorescence localization pattern identical to that of untreated embryos (Fig. 6A).

Labeling with FITC-phalloidin of cytochalasin D-treated embryos undergoing gastrulation showed a break-up of cortical fluorescence localization (Fig. 5A) compared with the continuous appearance of cortical fluorescence in non-treated embryos (Fig. 5B). This suggests that cytochalasin D was effective in penetrating embryos at these stages and effecting the disruption of F-actin.

On the ventral aspect of the 4-cell stage, confocal images (Fig. 6A-F) revealed orientated streams of cortical FITC-phalloidin staining, reflecting the distribution of F-actin, and forming a pattern that

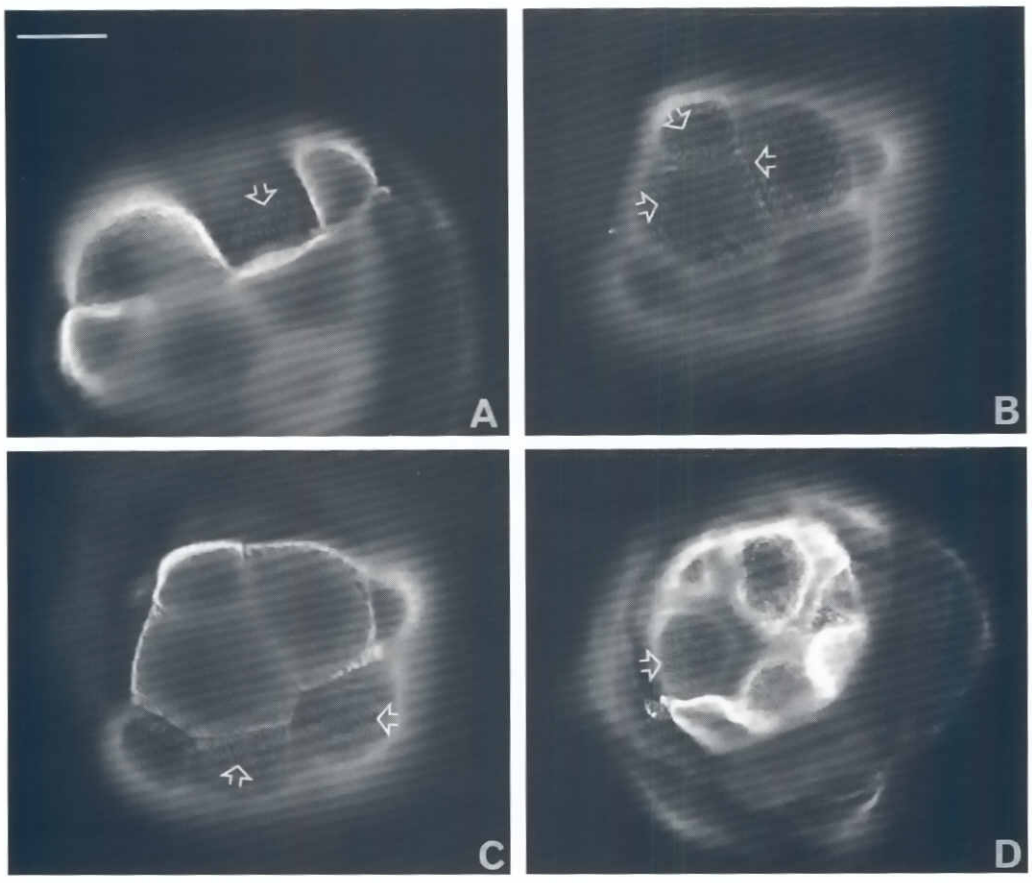

Figs. 4. Treatment with cytochalasin D for disruption of F-actin: effect on surface architecture. Vegetal surface of live eggs at gastrulating stages. **(A)** *No cytochalasin treatment. Embryos incubated in FITC-GSL-1 only. Surface architecture (arrowed) on cell in region commencing blastopore formation.* **(B-D)** *Embryos incubated simultaneously in cytochalasin D and FITC-GSL-1. Note localization of fluorescence to surface architecture, similar to that seen in embryos with no cytochalasin D treatment. Surface architecture (arrowed) on cells just prior to blastopore formation (Figs. 4B,C) and commencing blastopore formation (Fig. 4D). Bar, 20 μm.*

correlates with the lines of characteristic surface architecture in lobe-forming stages observed by confocal imaging with fluorescent lectins (Fig. 3A). Lines of FITC-phalloidin swirled in from the C cell towards the D cell (Fig. 6A); on the D cell, they started to diverge. Towards the left half of the D cell (appearing as right half ventrally) the lines passed upwards towards the polar furrow (Fig. 6B), curving towards the junction of the A, B and D cells. The lines sometimes anastomosed, and curved around a centre of radius (CR, Fig. 6C-D) on the D cell. Finally, the lines continued both on to the A cell and downwards over the D cell, where they diverged away (Fig. 6D).

Discussion

A detailed animal and vegetal region surface architecture on cleaving eggs of *Crepidula* has been observed and documented both by LT-SEM and lectin staining with confocal imaging microscopy. The localization of the characteristic «animal» surface architecture raises a number of points.

Firstly, the architecture appears to be organized around the animal-vegetal axis (Fig. 1A and B), which is spatially related to the anterior-posterior axis of the subsequent embryo. This is apparent, for example, on the $1q^1$ cells (daughter cells of the 1st quartet of micromeres) (Fig. 1A and B). Some lines (short arrows in Fig. 1B) originate from the animal pole, whilst others (long arrows in Fig. 1B) curve away from the pole. Thus the surface architecture may provide a visible marker reflecting a morphogenetic field involved in generating the a-p axis.

Animal/vegetal polarity in most mollusc eggs arises initially from the position of the oocyte in the ovary. Raven (1963,1967) observed that the apicobasal axis of the *Lymnaea* oocyte corresponds with the later animal-vegetal axis of the egg. He assumed that this contact region results in the "imprinting" of special properties in the future vegetal pole surface. Regional differences in membrane properties (such as electrical excitability) related to the polar axis have indeed been shown to exist in De*ntalium* eggs (Jaffe and Guerrier, 1981). The large surface area, produced by the ridges of the animal region surface architecture, may facilitate maximum traffic of ions in this region. Such an influx has been demonstrated, at least in the vegetal region of *Bithynia* mollusc eggs (Zivkovic and Dohmen, 1991). The animal-vegetal architecture organization correlates well with the animal-vegetal polarity of an ionic current pattern measured with the vibrating probe in *Lymnaea stagnalis* in the uncleaved egg, during gastrulation and organogenesis, when the antero-posterior axis is forming (Zivkovic *et al.*, 1990; Creton *et al.*, 1993).

There has been a recent revival of interest in the field concept, which was first attributed to Driesch (1891). According to Goodwin (1984, 1985), a morphogenetic field is a spatial domain in which each part has a state determined by the state of neighboring parts so that the whole has a specific relational structure. Goodwin and Trainor (1985) proposed that mechano-chemical fields based on

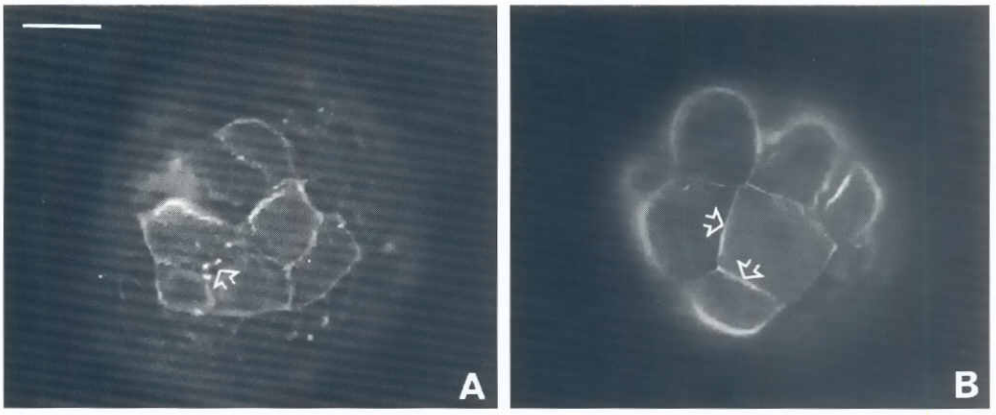

Figs. 5. Treatment with cytochalasin D: effect on cortical F-actin. *Vegetal aspect of embryos at gastrulating stages stained with FITC-phalloidin for location of F-actin.* **(A)** *Embryos incubated in cytochalasin D, then fixed, permeabilized and stained with FITC-phalloidin. Note break-up of cortical FITC-phalloidin (arrowed).* **(B)** *No cytochalasin D treatment. Uniform cortical FITC-phalloidin (arrowed).Bar, 20 μm.*

cytoskeletal-ionic interactions may provide the generative basis of morphogenesis. In vertebrate embryos, gradient fields can be visualized at the level of individual regulatory molecules (DeRobertis *et al.*, 1991). Beads soaked in fibroblast growth factors induce additional limb development in the flank of chick embryos, providing recent evidence for the existence of a morphogenetic field, with axial characteristics which generate limb identity (Cohn *et al.*, 1995). In the early amphobian embryo, a field may comprise a three dimensional coordinate system of internal voltages, which provides cues for polarity and morphogenesis (Shi and Borgens, 1995). A major contribution to field theories (Raven, 1966) relates to molluscs. Raven envisaged that the field, residing in the egg cortex, generated the body axes. He commented, "the cortical field has a general co-ordinating and integrating function in development. It has a polar structure, and is organized in dorso-ventral and transverse directions. It lays down the general plan of the embryo in broad outline." Agents which disrupt the body plan may act by interfering with the formation or maintenance of morphogenetic gradients. For instance the Li+ ion may perturb generation of a morphogenetic field by influencing a phosphoinositide signaling gradient (Berridge *et al.*, 1989), plasma membrane protein pattern (Lazou and Beis, 1993), microtubule polymerization (Bhattacharaya and Wolff, 1976) or membrane lipid composition (Lopez-Corcuera *et al.*, 1988). Having observed the surface architecture pattern, we now intend to investigate whether it is set up by electric currents, by perturbation with an applied electric field; or if it is controlled by spindle orientation, which can be disrupted by pressure experiments.

A second point of interest is that the architecture forms a pattern specific to each micromere quartet (formed sequentially during spiral cleavage), which comprises, in turn, the $1q^1$ cells, $1q^2$ cells, 2q and 2Q cells. This suggests that an underlying morphogenetic field may organize the cleavage pattern. As a more specific manifestation of such a field, the surface architecture on each specific micromere quartet unit may reflect the future developmental potential of that unit. Raven ascribed the determination of cleavage pattern to the influence of the cortical field. Lithium-treated Lymna*ea* eggs showed a reduction in micromere size, suggesting a displacement of the spindles towards the animal pole, which in turn may have been due to a disruption of the cortical field (Raven *et al.*, 1952).

The position of the centres of radii (CR) of the lines may have some morphogenetic significance. The CRs on the $1q^2$ cells are surrounded on their left, by a series of lines which curve dextrally as they progress outwards. It is conceivable that the alternating spiral cleavage movements are implicated in the generation of this surface pattern, or vice versa. Moreover, both the CRs and the parallel series of lines are not in precisely the same locations in each quadrant. Such precision may not be necessary if, for example, the role of the underlying morphogenetic field is only to locate the cells to their approximate position. It would be interesting to investigate if the CRs are signaling centres or hotspots, precise sites which initiate repetitive calcium waves (reviewed by Berridge and Dupont, 1994), such as the ER-plasma membrane-associated -cortical pacemaker- implicated in the development of axial form of ascidian eggs (Speksnijder, 1992).

Thirdly, the close correlation of the F-actin distribution with that observed both with FITC-lectins and by LT-SEM suggests that the F-actin is localized to the same architecture. This is the first demonstration of a localization of a cytoskeletal element to this surface architecture and may indicate a common role. These studies indicate that the integrity of F-actin is not responsible for the maintenance of the surface architecture, nor of the localization of GSL-1 to that architecture. This suggests that the F-actin and surface architecture are unconnected. The architecture found on the polar lobe-bearing region of eggs varies between gastropod taxa with different types of body form. It can be speculated that subtle distinctions in the vegetal surface architecture cortical F-actin complex might reflect, the nature of a morphogenetic field which may be important in the generation of type-specific form. If this is so, elucidation of the mechanism of development, and influence of this architecture could be crucial to an understanding of the generation of diversity within the Gastropoda.

In conclusion, the surface architecture of *Crepidula* eggs may provide a model for the study of a morphogenetic field system. If the nature and mode of action of this field can be identified, such knowledge could be of wider significance in understanding generative mechanisms in other molluscs, and possibly other phyla.

Materials and Methods

Crepidula fornicata

Specimens were dredged from Plymouth Sound by the Marine Biological Association, Plymouth, and were obtained intertidally at Hillhead, 4m W of Portsmouth (SU 540 020). They were kept in running seawater pumped through a fiberglass filter and over cooling plates to maintain a water

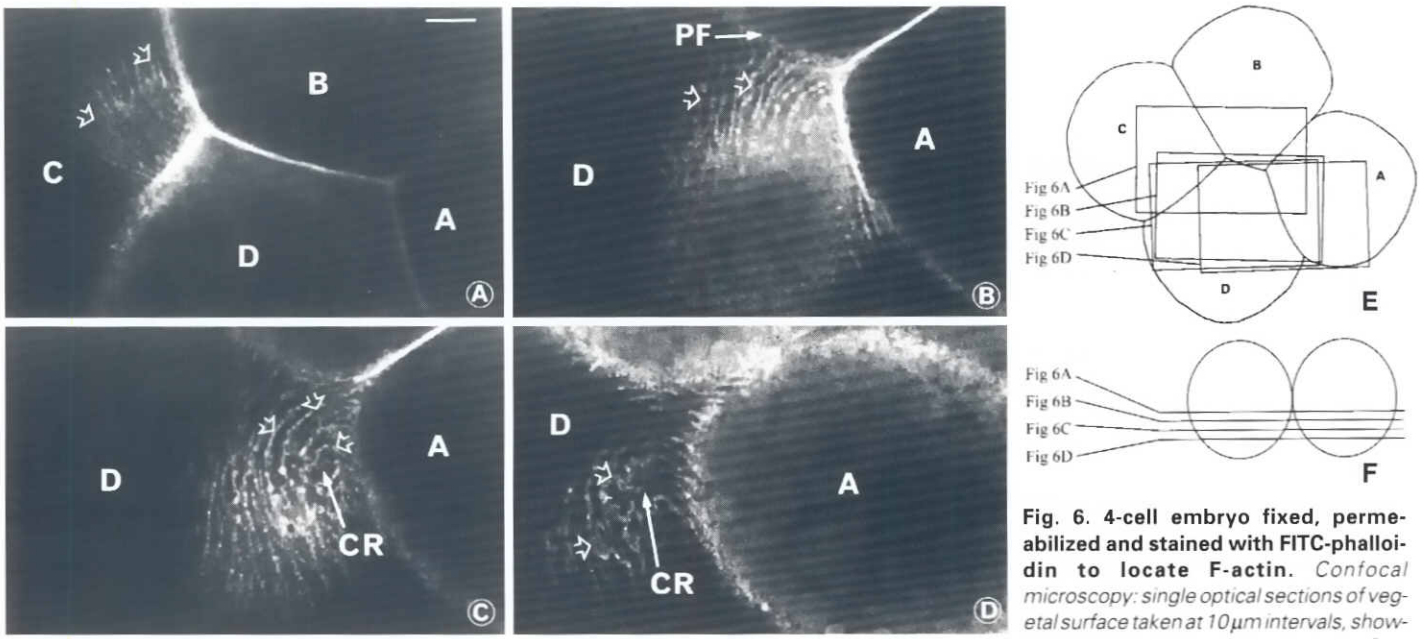

Fig. 6. 4-cell embryo fixed, permeabilized and stained with FITC-phalloidin to locate F-actin. *Confocal microscopy: single optical sections of vegetal surface taken at 10 μm intervals, showing distinct pattern of F-actin lines. Successive images 6A-D progress from vegetal surface towards animal region. Letters denote A, B, C and D cells.* **(A)** *First image of incremental series. Lines (open arrows) on C cell swirling towards D cell.* **(B)** *Lines (open arrows) on D cell passing up towards polar furrow (PF) and curving towards junction of A, B and D cells.* **(C)** *Lines (open arrows) on D cell curving around centre of radius (CR).* **(D)** *Lines (open arrows) on D cell passing on to A cell. Note anastomosing of lines in CR region. Bar, 15 μm.* **(E)** *Diagram of vegetal surface at 4-cell stage. Boxed areas denote approximate fields of view shown in Figures 6A-6D.* **(F)** *Diagram of side view of embryo in Figure 6E, denoting plane of optical sections shown in Figs. 6A-6D and their relative position (not to scale).*

paraformaldehyde in a buffer containing 100 mM KCl, 5 mM magnesium acetate (Sigma), 5 mM EGTA (ethylene glycol-bis [B-aminoethylether] N,N,N',N'-tetraacetic acid),(Sigma), and 10 mM PIPES (piperazine-N,N'-bis [2-ethanesulphonic acid]) (pH 6.8) (Sigma) to which 300 mM sucrose was added. The embryos were then washed in buffer, extracted for 5 min in 0.5% Nonidet P-40 (Sigma) in buffer, rinsed in buffer and incubated for 1 h in 0.3 μg/ml FITC-Phallacidin (Sigma), in buffer diluted from a stock solution of 20 μg/ml in buffer stored at 4°C. The embryos were given a final buffer wash before examination.

Fluorescence microscopy

Embryos were mounted on microscope slides with 200 μm spacers on which a coverslip was overlaid. The incidence and distribution of fluorescence was viewed on a Zeiss microscope fitted with a Biorad MRC 600 confocal scanhead with a 15 mW argon laser which emits 2 lines, at 488 nm and 514 nm. The filters were calibrated for FITC and rhodamine; BHS and GHS filter sets were used to image the FITC and rhodamine fluorescence with both laser lines. Pinholes were set between 5 and 6 mm. Images were stored as Bio-rad's own Pic format and recorded onto Ilford FP4 film through a monitor screen-mounted Nikon F301 camera. For the animal region surface architecture (Fig. 1), a Z-series of 12 images of the embryo surface was collected at 5 μm intervals, using an Olympus 10x0.3 NA objective (S plan 10) which was further magnified 2 times. For the polar lobe surface architecture (Fig. 5), a single image was obtained using a Kalman filter (average of 5) with a Zeiss 16x0.5 objective which was further magnified 4 times. For the observation of cortical F-actin distribution (Fig. 6A-D), a single image was obtained using a Kalman filter (average of 5) with a Nikon 60x1.4 oil objective which was further magnified 1.5 times.

Treatment with cytochalasin D

Cytochalasin D disrupts the organization of polymerized actin (Schliwa, 1982). Embryos were incubated either in 1 μg/ml cytochalasin D in filtered temperature below 10°C to prevent egg laying. Animals were fed two or three times per week with Liquifry Marine (Liquifry Co. Ltd.) and egg-laying was induced by transferring animals to water between 12-17°C. The adult female *Crepidula fornicata* remains in contact with her laid eggs, which are attached to the substratum or underlying animal, so the shell must be prised off to obtain the eggs. Very careful reposition of the female back into its site of attachment often enabled the disturbed animal to remain viable and occasionally lay again. The capsules were dissected with fine scissors to remove the eggs.

Fluorescent lectins

Selected live embryonic stages of *Crepidula* were incubated in 100 μg/ml FITC-conjugated *Griffonia(Bandeirea) simplicifolia* lectin-1 (GSL-1) in filtered seawater containing 0.075% sodium azide and 1% bovine serum albumen (BSA) [AB-FSW] at 12-17°C for 2 h and then rinsed extensively in AB-FSW. The medium included sodium azide in order to inhibit energy-dependent patching of bound lectin and BSA to provide a physically protective protein layer and prevent non-specific protein adsorption to the membrane throughout the procedure. Control embryos were incubated without FITC-GSL-1, or incubated with FITC-GSL-1 concurrently with the sugar to which it binds (α-D galactose). The sugar concentration was chosen to be in excess of that necessary to saturate lectin binding. Omission of FITC-GSL-1 revealed any autofluorescence, which was found to be negligible. Adding competing monosaccharide with the lectin provided a control for sugar specificity, in which case negligible fluorescence was also observed.

Distribution of microfilaments

F-actin was visualized by treatment with FITC-Phallacidin, a derivative of Phalloidin, which binds to and stabilizes filamentous actin (Wieland and Faultish, 1978; Barak *et al.*, 1980). The protocol followed was that of Speksnijder *et al.* (1991). Embryos were fixed for 10 min in 4%

seawater containing 1% BSA for 90 min or in this solution for 30 min and then simultaneous incubation in cytochalasin D and FITC-GSL-1 for 60 min The effect of cytochalasin D upon the distribution of GSL-1 binding sites was then examined by fluorescence microscopy. The effect of cytochalasin D upon the distribution of F-actin was examined by extraction, fixation and immunocytochemistry as described for microfilaments above.

Low temperature SEM

Eggs were fixed in 2.5% (v/v) glutaraldehyde made up in FSW, pH 7.2, for 15 min and washed extensively in distilled water to remove post-freezing cell surface salt crystal accumulation. Eggs were transferred in a drawn-out Pasteur pipette onto a specimen stub. To retain the eggs upon the stub at all tilt angles, the stubs were washed in detergent and coated with 0.1% (w/v) poly-L-lysine (Sigma), a cationic polypeptide adhesive. To obviate excessive sublimation times, eggs of each species were left on the stub at RT, until each egg was almost devoid of surrounding water (c.a. 2 min at 20°C). Eggs were frozen in nitrogen slush then transferred to a Leica Cambridge 200 SEM fitted with an Oxford Instruments low temperature stage. The specimen was heated to -80°C to sublime ice from the egg surface and subsequently sputtered with gold in the cryo prechamber in 6x30 sec bursts, at 5 min intervals. The specimen temperature was maintained between -160°C and -165°C. Images were recorded as for TEM.

Acknowledgments

The authors are thankful for assistance from Grenham Ireland (confocal imaging); Tony Bentley, Les Lockey and Ian Miller (photography); and the staff of the electron microscope unit. The research was funded by a Science and Engineering Research Council UK Instant Award.

References

BARAK, L.S., YOKUM, R.R., NOTHNAGEL, E.A. and WEBB, W.W. (1980). Fluorescence staining of the actin cytoskeleton in living cells with 7-nitrobenz-2-oxa-1,3-diazole phallacidin. *Proc. Natl. Acad. Sci. USA 77*: 980- 984.

BERRIDGE, M.J. and DUPONT, G. (1994). Spatial and temporal signalling by calcium. *Curr. Opin. Cell Biol. 94*: 267-274.

BERRIDGE, M.J., DOWNES, C.P. and HANLEY, M.R. (1989). Neural and developmental actions of Lithium - a unifying hypothesis. *Cell 59*: 411-419.

BHATTACHARAYA, B. and WOLFF, J. (1976). Stabilization of microtubules by lithium ion. *Biochem. Biophys. Res. Commun. 73*: 383-390.

COHN, M.J. IZPISUA-BELMONTE, J.C., ABUD, H., HEATH, J.K. and TICKLE, C. (1995). Fibroblast Growth Factors Induce Additional Limb Development from the Flank of Chick Embryos. *Cell 80*: 739-746.

CRAIG, M.M. and MORRILL, J.B. (1986). Cellular arrangements and surface topography during early development in embryos of *Ilyanassa obsoleta*. *Int. J. Invert. Reprod. Dev. 9*: 209-228.

CRETON, R., ZIVKOVIC, D., ZWAAN, G. and DOHMEN, M.R. (1993). Polar ionic currents around embryos of *Lymnaea stagnalis* during gastrulation and organogenesis. *Int. J. Dev. Biol. 37*: 425-431.

DEROBERTIS, E.M., MORITA, E.A. and CHO, K.W.Y. (1991). Gradient fields and homeobox genes. *Development 112*: 669-678.

DOHMEN, M.R. (1992). Cell lineage in molluscan development. *Micros. Res. Tech. 22*: 75-102.

DOHMEN, M.R. and VAN DER MEY, J.C.A. (1977). Local surface differentiations at the vegetal pole of the eggs of *Nassarius reticulatus*, *Buccinum undatum*, and *Crepidula fornicata*. (Gastropoda, Prosobranchia), *Dev. Biol. 61*: 104-113.

DREISCH, H. (1891). Entwicklungsmechanische Studien I-II. *Z. Wiss. Zool. 53*: 160-182.

GOODWIN, B.C. (1984). A relational or field theory of reproduction and its evolutionary implications. In *Beyond Neo-Darwinism* (Eds M.W. Ho & P.T. Saunders), Academic Press, London, pp. 234-241.

GOODWIN, B.C. (1985). The causes of morphogenesis. *Bioessays 3*: 32-36.

GOODWIN, B.C. and TRAINOR, L.E.H. (1985). Tip and whorl morphogenesis in *Acetabularia* by calcium-regulated strain fields. *J. Theor. Biol. 117*: 79-106.

JAFFE, L.A. and GUERRIER, P. (1981). Localisation of electrical excitability in the early embryo of *Dentalium*. *Dev. Biol. 83*: 370-373.

LAZOU, A. and BEIS, A. (1993). Lithium induces changes in the plasma membrane protein pattern of early amphibian embryos. *Biol. Cell 7*, 265-268.

LOPEZ-CORCUERA, B., GIMENEZ, C. and ARAGON, C. (1988). Change of synaptic membrane lipid composition and fluidity by chronic administration of lithium. *Biochim. Biophys. Acta 939*: 467-475.

NUCCITELLI, R. (1984). The involvement of transcellular ion currents and electric fields in pattern formation. In *Pattern Formation* (Eds. G.M. Malacinski & S.V. Bryant), Macmillan Publishing Company, New York. pp: 23-46.

NUCCITELLI, R. (1988). Ionic current in morphogenesis. *Experientia 44*: 657- 666.

RAVEN, C.P. (1963). The nature and origin of the cortical morphogenetic field in *Limnaea*. *Dev. Biol. 7*: 130-143.

RAVEN, C.P. (1966). *Morphogenesis: the Analysis of Molluscan Development.* Pergamon Press, London.

RAVEN, C.P. (1967). The distribution of special cytoplasmic differentiations of the egg during early cleavage in *Limnaea stagnalis*. *Dev. Biol. 16*: 407-437.

RAVEN, C.P., BEZEM, J.J. and ISINGS, J. (1952). Changes in the size relations between macromeres and micromeres of *Limnaea stagnalis* under the effect of lithium. *Proc. Kon. Ned. Akad. V. Wetensch. Amst. 55*, 248-258.

SCHLIWA, M. (1982). Action of cytochalasin D on cytoskeletal networks. *J. Cell Biol. 90*: 222-235.

SHI, R. and BORGENS, R.B. (1995). Three-dimensional gradients of voltage during development of the nervous system as invisible coordinates for the establishment of embryonic pattern. *Dev. Dynamics 202*: 101-114.

SPEKSNIJDER, J.E. (1992). The repetitive calcium waves in the fertilized ascidian egg are initiated near the vegetal pole by a cortical pacemaker. *Dev. Biol. 153*: 259-271.

SPEKSNIJDER, J.E., TEERDS, K.J., HAGE, W.J. and DOHMEN, M.R. (1991). Polar effects of concanavalin A on the cortical cytoskeleton of a molluscan egg (*Nassarius reticulatus*, Gastropoda). *Roux's Arch. Dev. Biol. 200*: 8-20.

VAN DEN BIGGELAAR, J.A.M. and GUERRIER, P.(1983). Origin of spatial information. In *The Mollusca: Volume 3. Development* (Eds. N.H. Verdonk, J.A.M. Van den Biggelaar & A.S. Tompa), Academic Press, New York, pp.179-213.

VERDONK, N.H. and CATHER, J.N. (1983). Morphogenetic determination and differentiation. In *The Mollusca 3*: 215-252.

WIELAND, T. and FAULTISH, M. (1978). Amatoxin, phallolysin, and antaminide: the biologically active components of poisonous *Amantia* mushrooms. *CRC Crit. Rev. Biochem. 5*, 185-260. Cited in *Developmental Biology, a Comprehensive Synthesis: Volume 2. The Cellular Basis of Morphogenesis* (Ed. W. Browder), pp.3-29. Plenum Press, New York (1986).

ZIVKOVIC, D. and DOHMEN, M.R. (1991). Changes in transcellular ionic currents associated with cytokinesis and polar lobe formation in embryos of *Bithynia tentaculata* (Mollusca). *Development 112*: 451, 459.

ZIVKOVIC, D. CRETON, R., ZWAAN, G., DE BRUIJN, W.C. and DOHMEN, M.R. (1990). Polar localization of plasma membrane Ca^{2+}/Mg^{2+} ATPase correlates with the pattern of steady ionic currents in eggs of *Lymnaea stagnalis* and *Bithynia tentaculata* (Mollusca). *Roux's Arch. Dev. Biol. 199*: 134-145.

Received: June 1996

Accepted for publication: October 1997